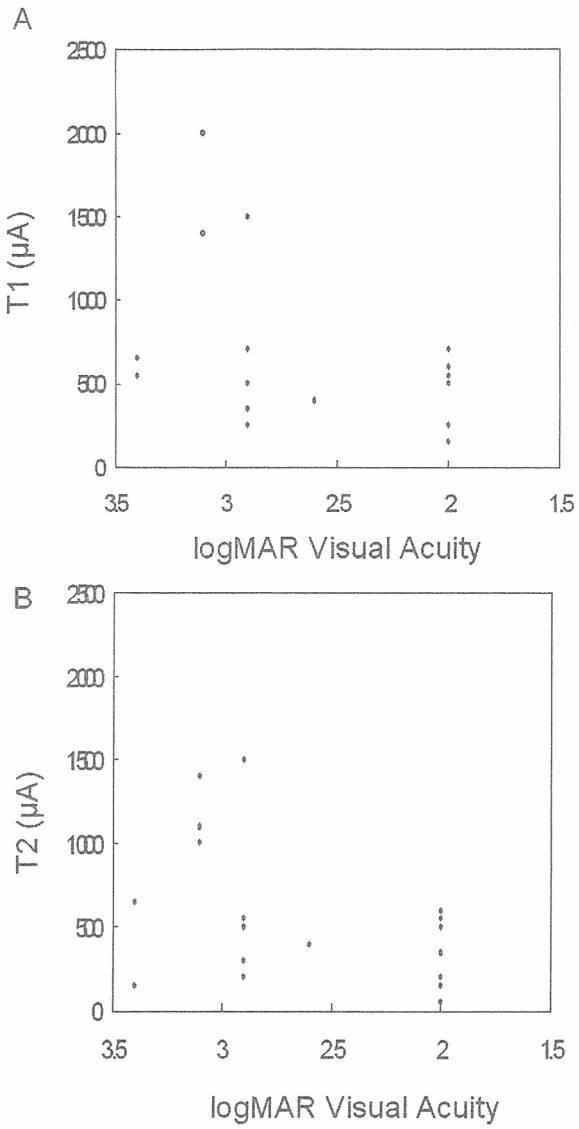

Fig. 3 Relationship between T1 and T2 and logMAR visual acuities in patients. **a**. T1s are plotted versus logMAR visual acuities, **b**. T2s are plotted versus logMAR visual acuities. There was no significant correlation between thresholds and logMAR visual acuities

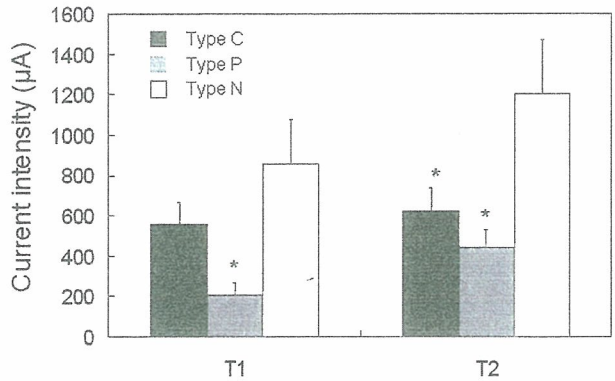

Fig. 4 Comparison of the type of residual visual fields with thresholds of phosphene. Type C; central visual field preserved within a 30° radius; type P, peripheral visual field left outside the central 30°; type N; complete loss of visual field. Data were presented as mean±SEM. There was a significant difference between three thresholds (one-way ANOVA: T1, T2; $P<0.05$; Tukey test, * $P<0.05$ vs type N)

mean current intensity of T2 in the RP patients was higher than in the CRD patients, the difference was not significant (790±126 μA vs 440±91 μA).

Relationship between pupillary responses and thresholds in RP patients

An EEPR was examined in all but three RP patients. These three had nystagmus and the tests for an EEPR could not be performed, and they were excluded from the analysis. An EEPR was recorded from all eyes with CRD, but 54% (7/13) of the RP eyes did not show a positive EEPR (Fig. 6a).

The RP patients were classified into four groups on the basis of the presence or absence of a light and electrically-elicited pupillary response: type I, 15% (2/13) had light reflex (+) and EEPR (+); type II, 31% (4/13) had no light reflex (−) and had an EEPR (+); type III, 23% (3/13) had light reflex (+) and no EEPR (−); and type IV, 31% (4/13) had no light reflex (−) and no EEPR (−).

The waveform of the EEPR was very similar to that of the light response (Fig. 6a).

We examined the relationship between EEPR and thresholds of phosphenes in RP patients. We compared the thresholds of RP eyes that had a EEPR to those who did not have a EEPR. The absence or presence of EEPR completely divided patients into high or low thresholds groups. In the group with an EEPR, the mean current intensity of T1 was 400±62 μA, and the mean intensity of T2 was 433±75 μA. On the other hand, in the group without an EEPR, the mean intensities of T1 and T2 were significantly increased to 921±169 μA and 1,179±203 μA, respectively (T1, $P<0.05$; T2, $P<0.01$; Fig. 6b).

Side effects of TES examination

During the TES examination, no subjects complained pain or irritable sensation on cornea or upper lid. The slit-lamp examination after TES examination revealed a slight superficial punctuate keratopathy in all cases, which was comparable to those observed after the routine examination of electro-retinography.

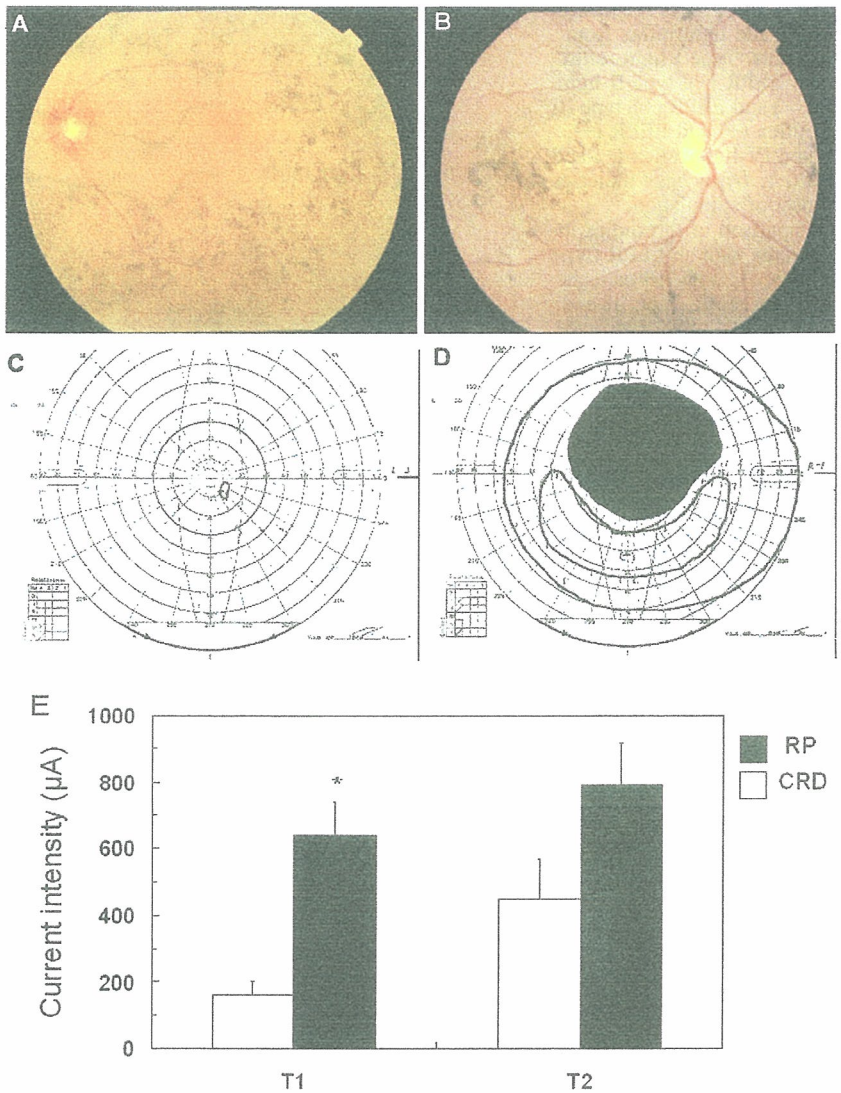

Fig. 5 Comparison of mean thresholds of RP patients with those of CRD patients. Representative fundus photographs and visual fields from two types of patients; **a** and **c** from a RP patient, **b** and **d** from a CRD patients. **e**. Mean thresholds of phosphene in two types of patients. There was a significant difference of T1 between the two groups (*, Mann-Whitney *U*-test, $P<0.05$); however, there was no significant difference in T2 between them

Discussion

Except a slight superficial punctuate keratopathy, no side effect was observed during or after TES, indicating that TES is a safe examination when performed along with our protocol.

The computer simulation showed that the charge density in the peripheral retina was higher than in the central retina if an eye was stimulated by a concentric corneal electrode [14], which was consistent with the observation that T2 was larger than T1. In order to elicit EEPR, more current was needed, suggesting that a more number of RGS should be involved to elicit pupillary reflex than to perceive phophene (Fig. 1).

A possibility that a direct current affected the pupil efferent and elicited the EEPR was neglected by the report that in eyes of optic atrophy, EEPR was not induced in the contra lateral healthy eye [32].

All RP patients perceived a phosphene, but the average threshold current of T1 or T2 was 7–8 times greater in RP patients than in normal subjects, suggesting that the number of residual RGC was much smaller in RP patients than in normal subjects [9, 27]. (Fig. 1). The threshold current of phosphenes varied among the patients, indicated that the residual RGCs function varied among patients (Table 2).

A plot of T1 and T2 in normal subjects and patients showed two groups. In one group, T2 was highly correlated with T1 as in normal subjects, and in the other group, the T2 was elevated relative to T1 (Fig. 2). These results indicate that in the former group, the rate of RGC loss in macula area may be similar to that in the extramacular area as reported [9, 27, 29], while in the latter group, the degree of RGC loss in the macula may be higher than that in the extramacular area.

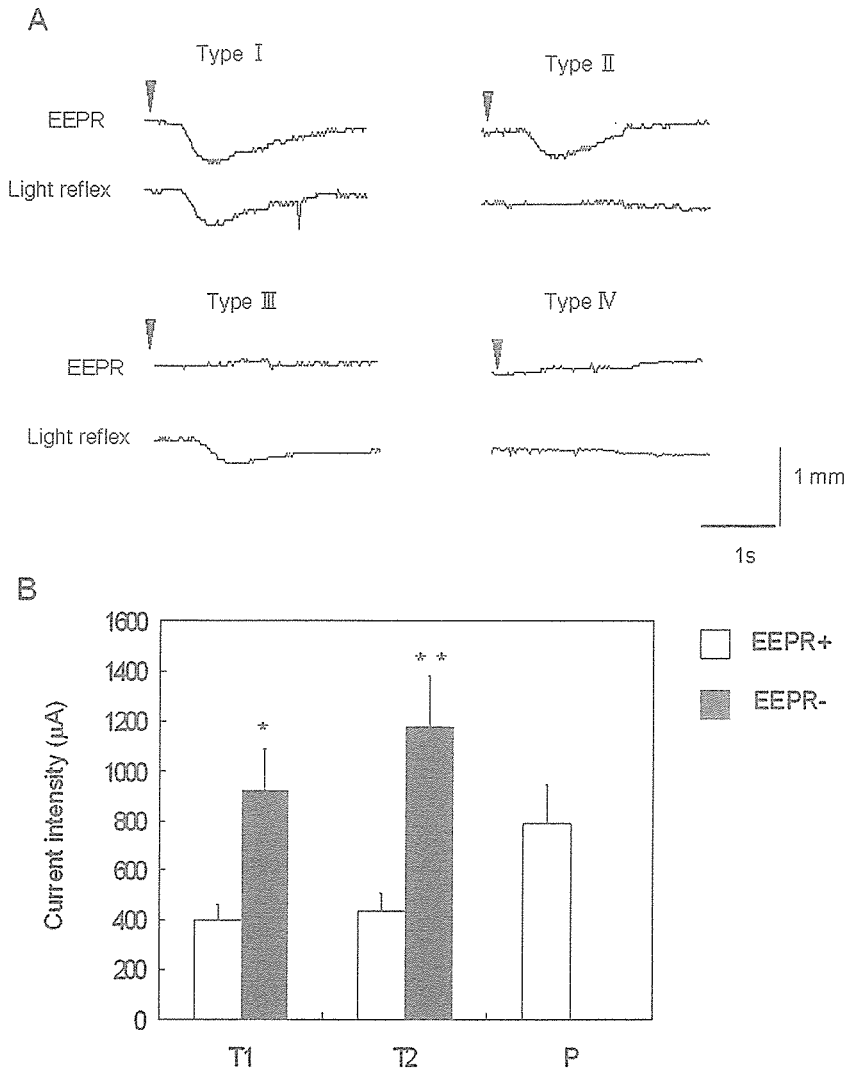

Fig. 6 a. Four types recordings of EEPR and light reflex from RP patients. Type I light reflex (+) and EEPR (+), type II light reflex (−) and EEPR (+), type III light reflex (+) and EEPR (−), and type IV light reflex (−) and EEPR (−). *Arrow head* indicates the onset of stimulation. b. Comparison of thresholds in RP patients with an EEPR (type I and type II) with RP patients without an EEPR (type III and type IV) There were significant differences between patients with an EEPR and without an EEPR (student *t*-test: T1; **P*<0.05, T2; ***P*<0.01)

We also found that the threshold of phosphenes and logMAR visual acuity were not significantly correlated. The thresholds of blind patients were lower than those of some patients who were not blind (Fig. 3). These findings indicate that threshold of phosphenes rather than the visual acuity may be a better indicator of the residual RGC function in patients with severe retinal degeneration.

We further compared the thresholds in the group with a preservation of the central visual field left to those with a preservation of the peripheral visual field. Although the mean T1 threshold in the central visual field group was higher than that in peripheral visual field group, the mean T2 threshold in the central visual field group was not lower but higher than that in peripheral visual field group in spite of the remaining of the center of visual field (Fig. 4). Thus, the RGCs in the central retina were preserved more in the peripheral visual field group than in the central visual field group.

The mean current intensity of T1 and T2 in CRD patients was lower than those in RP patients (Fig. 5e), suggesting that the RGC function were more preserved in CRD patients than in RP patients in both the macula and extramacular areas.

Although all CRD patients showed a positive EEPRs, all RP patients did not show them. Moreover thresholds of phosphenes varied among RP patients. There were significant differences between the T1 and T2 for the group with an EEPR and those without an EEPR (Fig. 6). The presence or absence of EEPR is a good indicator of the extent of residual RGC function in patients with retinal degeneration.

On the contrary, the mean threshold of EEPR was twice as high as that of T2 in the group with an EEPR, although the thresholds of T2 and EEPR were close in normal subjects. Thus the thresholds of EEPR would not be a good indicator of the central phosphene in RP patients. A certain number of RGCs may have to be functioning to evoke a

pupillary constriction. However, in advanced RP patients, the density of RGC is so low that a higher current is needed to depolarize the widely scattered RGCs to evoke a pupillary constriction, while phosphene may be perceived even if a small number of RGCs were depolarized by TES.

These data suggest that three parameters, T1, T2 and P, measured by TES examination can be used to select candidates for retinal prostheses.

In summary, we have developed a safe method to elicit phosphenes and EEPR by TES to study the residual RGC function in patients with retinal degeneration. In RP patients, the presence of EEPR did not necessarily indicate the preservation of RGCs in the central retina, but reflected the overall activity of residual RGCs. Therefore, our method may provide information on the function of residual RGC which cannot be examined with currently available ophthalmologic instruments. Thus, among several tests required to select candidates for a retinal prosthesis [35],TES may have an important role.

Acknowledgements The authors thank Yozo Miyake, Satoshi Suzuki, Mineo Kondo and Yutaka Fukuda for advice and discussions.

References

1. Brindley GS (1955) The site of electrical excitation of the human eye. J Physiol 127:189–200
2. Chow AY, Chow VY (1997) Subretinal electrical stimulation of the rabbit retina. Neurosci Lett 225:13–16
3. Chow AY, Chow VY, Packo KH, Pollack JS, Peyman GA, Schuchard R (2004) The artificial silicon retina microchip for the treatment of vision loss from retinitis pigmentosa. Arch Ophthalmol 122:460–469
4. Delbeke J,Pins D, Michaux G, Wanet-Defalque MC, Parrini S, Veraart C (2001)Electrical stimulation of anterior visual pathways in retinitis pigmentosa. Invest Ophthalmol Vis Sci 42:291–297
5. Fariss RN, Li ZY, Milam AH (2000) Abnormalities in rod photoreceptors, amacrine cells, and horizontal cells in human retinas with retinitis pigmentosa. Am J Ophthalmol 129:215–223
6. Gebhard JW (1952) Thresholds of the human eye for electric stimulation by different wave forms. J Exp Psychol 44:132–140
7. Haruta M, Kosaka M, Kanegae Y, Saito I, Inoue T, Kageyama R, Nishida A, Honda Y, Takahashi M (2001) Induction of photoreceptor-specific phenotypes in adult mammalian iris tissue. Nat Neurosci 4:1163–1164
8. Hesse L, Schanze T, Wilms M, Eger M (2000) Implantation of retina stimulation electrodes and recording of electrical stimulation responses in the visual cortex of the cat. Graefe's Arch Clin Exp Ophthalmol 238:840–845
9. Humayun MS, Price M, de Juan Jr E, Barron Y, Moskowitz M, Klock IB, Milam AH (1999) Morphometric analysis of the extramacular retina from postmortem eyes with retinitis pigmentosa. Invest Ophthalmol Vis Sci 40:143–148
10. Humayun MS, Weiland JD, Fujii GY, Greenberg RJ, Williamson R, Little J, Mech B, Climmarusti V, Van Boemel G, Dagnelie G, de Juan Jr E (2003) Visual perception in a blind subject with a chronic microelectronic retinal prosthesis. Vision Res 43:2573–2581
11. Jensen RJ, Rizzo JF 3rd, Ziv OR, Grumet A, Wyatt J (2003) Thresholds for activation of rabbit retinal ganglion cells with an ultrafine, extracellular microelectrode. Invest Ophthalmol Vis Sci 44:3533–3543
12. Johnson LN, Guy ME, Krohel GB, Madsen RW (2000) Levodopa may improve vision loss in recent-onset, nonarteritic anterior ischemic optic neuropathy. Ophthalmology 107: 521–526
13. Kanda H, Morimoto T, Fujikado T, Tano Y, Fukuda Y, Sawai H (2004) Electrophysiological studies on the feasibility of suprachoroidal-transretinal stimulation for artificial vision in normal and RCS rat. Invest Ophthalmol Vis Sci 45:560–566
14. Kawasumi M (1985) Distribution of current intensities inside the electrically stimulated eye. Nippon Ganka Gakkai Zasshi 89:766–772
15. Li ZY, Kjavin IJ, Milam AH. (1995) Rod photoreceptor neurite sprouting in retinitis pigmentosa. J Neurosci 15:5429–5438
16. Majji AB, Humayun MS, Weiland JD, Suzuki S, D'Anna SA, de Juan Jr E (1999) Long-term histological and electrophysiological results of an inactive epiretinal electrode array implantation in dogs. Invest Ophthalmol Vis Sci 40:2073–2081
17. Margalit E, Maia M, Weiland JD, Greenberg RJ, Fujii GY, Torres G, Piyathaisere DV, O'Hearn TM, Liu W, Lazzi G, Dangnelie G, Scribner DA, de Juan Jr E, Humayun MS (2002) Retinal prosthesis for the blind. Surv Ophthalmol 47:335–356
18. Marmor MF, Aguirre G, Arden G (1983) Retinitis pigmentosa: a symposium on terminology and methods of examination. Ophthalmology 90: 126–131
19. Motokawa K, Iwama K (1950) Resonance in electrical stimulation of the eye. Tohoku J. Exp Med 53:201–206
20. Motokawa K, Ebe M (1952) Selective stimulation of color receptors with alternating currents. Science 25:115:92–94
21. Miyake Y, Yanagida K, Yagasaki K (1980) Clinical application of EER (electrically evoked response). (1) Analysis of EER in normal subjects. Nippon Ganka Gakkai Zasshi 84: 354–360
22. Miyake Y, Yanagida K, Yagasaki K (1980) Clinical application of EER (electrically evoked response) (2) Analysis of EER in patients with dysfunctional rod or cone visual pathway. Nippon Ganka Gakkai Zasshi 84:502–509

23. Pagon RA (1988) Retinitis pigmentosa. Surv Ophthalmol 33:137–177
24. Potts AM, Inoue J (1968) The electrically evoked response of the visual system (EER). Invest Ophthalmol 7:269–278
25. Potts AM, Inoue J (1969) The electrically evoked response of the visual system (EER) II. Effect of adaptation and retinitis pigmentosa. Invest Ophthalmol 8:605–613
26. Rizzo JF 3rd, Wyatt J, Loewenstein J, Kelly S, Shire D (2003) Perceptual efficacy of electrical stimulation of human retina with a microelectrode array during short-term surgical trials. Invest Ophthalmol Vis Sci 44: 5362–5369
27. Santos A, Humayun MS, de Juan E Jr, Greenberg RJ, Marsh MJ, Klock IB, Milam AH (1997) Preservation of the inner retina in retinitis pigmentosa: a morphometric analysis. Arch Ophthalmol 115:511–515
28. Schwahn HN, Gekeler F, Kohler K, Kobuch K, Sachs HG, Schulmeyer F, Jacob W, Gabel VP, Zrenner E (2001) Studies on the feasibility of a subretinal visual prosthesis: data from Yucatan micropig and rabbit. Graefe's Arch Clin Exp Ophthalmol 239:961–967
29. Stone JL, Barlow WE, Humayun MS, de Juan E Jr, Milam AH (1992) Morphometric analysis of macular photoreceptors and ganglion cells in retinas with retinitis pigmentosa. Arch Ophthalmol 110:1634–1639
30. Tanino T, Kato S, Kawasumi M (1981) Studies on electrically evoked pupillary reflex-Indirect reflex and its frequency characteristics. Jpn J Ophthalmol 25:423–429
31. Tanino T, Kurihara K (1982) Electrically evoked direct and consensual reflexs of the pupil. Jpn J Ophthalmol 26:462–467
32. Tanino T. (1982) Studies on electrically evoked pupillary reaction 1. Indirect electrical reaction and its frequency characteristic. Nippon Ganka Gakkai Zasshi (Japanese) 61:397–402
33. Veraart C, Raftopoulos C, Mortimer JT, Delbeke J, Pins D, Michaux G, Vanlierde A, Parrini S, Wanet-Defalque MC (1998) Visual sensations produced by optic nerve stimulation using an implanted self-sizing spiral cuff electrode. Brain Res 813:181–186
34. Walter P, Heimann K (2000) Evoked cortical potentials after electrical stimulation of the inner retina in rabbits. Graefe's Arch Clin Exp Ophthalmol 238:315–318
35. Yanai D, Lakhanpal RR, Weiland JD, Mahadevappa M, Van Boemel G, Fujii G, Greenberg R, Caffey S, de Juan Jr E (2003) The value of preoperative tests in the selection of blind patients for a permanent microelectronic implant. Trans Am Ophthalmol Soc 101: 223–230
36. Young MJ, Ray J, Whiteley RS, Klassen H, Gage FH (2000) Neuronal differentiation and morphological integration of hippocampal progenitor cells transplanted to the retina of immature and mature dystrophic rats. Mol Cell Neurosci 16:197–205

Jpn J Ophthalmol 2006;50:266–273

DOI 10.1007/s10384-005-0304-y

CLINICAL INVESTIGATION

Effect of Transcorneal Electrical Stimulation in Patients with Nonarteritic Ischemic Optic Neuropathy or Traumatic Optic Neuropathy

Takashi Fujikado[1], Takeshi Morimoto[1], Kenji Matsushita[2], Hiroshi Shimojo[2], Yoshitaka Okawa[1], and Yasuo Tano[2]

[1] Department of Applied Visual Science, Osaka University Graduate School of Medicine, Osaka, Japan; [2] Department of Ophthalmology, Osaka University Graduate School of Medicine, Osaka, Japan

Abstract

Purpose: To determine whether transcorneal electrical stimulation (TES) can improve the visual function of patients with nonarteritic ischemic optic neuropathy (NAION) or traumatic optic neuropathy (TON).

Methods: Eight consecutive patients at the Osaka University Hospital were studied. TES (600–800 μA, 20 Hz, 30 min) was applied once each to three eyes with NAION and to five eyes with TON, using a contact lens-type stimulating electrode. The primary outcome measurement was the change in visual acuity at 1 to 3 months after TES. An improvement in visual acuity was defined as a change of ≥0.3 log (minimum angle of resolution) (logMAR) units. The side effects of TES were also investigated.

Results: After TES application, the visual acuity improved in two patients with NAION and in four patients with TON. Visual acuity did not worsen in any of the eyes. Only a mild superficial punctuate keratopathy was observed in all eyes immediately after TES, and it healed by the next day.

Conclusions: Visual acuity can be improved after TES without major complications in some patients with NAION or TON. These results suggest that TES should be considered as a new treatment for eyes with optic neuropathy. **Jpn J Ophthalmol** 2006;50:266–273 © Japanese Ophthalmological Society 2006

Key Words: contact lens, electrical stimulation, neuroprotection, nonarteritic anterior ischemic neuropathy, traumatic optic neuropathy

Introduction

Nonarteritic ischemic optic neuropathy (NAION) and traumatic optic neuropathy (TON) are optic nerve diseases accompanied by a sudden decrease in vision.[1] The visual decrease is often severe, and there is no established treatment that can reverse the decrease.[1] The natural course of the changes in visual acuity in eyes with NAION was documented by the Ischemic Optic Neuropathy Decompression Trial (IONDT) study.[2] The percentage of patients with a recovery of ≥3 lines, 0.3 log (minimum angle of resolution) (logMAR) in visual acuity, was 39.7% at 3 months in a carefully followed-up group, but the visual acuity gradually decreased during the remainder of the follow-up period. The natural course of the visual recovery in eyes with TON was documented by the International Optic Nerve Trauma Study (IONTS).[3] The percentage of untreated patients with a recovery of ≥3 lines in visual acuity was 57% at 1 month and 50% at 3 months.

The definitive cause of NAION is unknown, but optic nerve head ischemia secondary to hypoperfusion by the short posterior ciliary arteries is suspected.[4] The IONDT study reported that optic nerve decompression surgery was not effective for treating NAION.[5] Recent studies have

Received: July 29, 2005 / Accepted: December 19, 2005
Correspondence and reprint requests to: Takashi Fujikado, Department of Applied Visual Science, Osaka University Graduate School of Medicine, 2-2 Yamadaoka, Suita, Osaka 565-0871, Japan
e-mail: fujikado@ophthal.med.osaka-u.ac.jp

6. Kelly PJ, Weiter JJ. Resolution of optic disc neovascularization associated with intraocular inflammation. Am J Ophthalmol 1980; 90:545–548.
7. Semple HC, Landers MB, Morse LS. Optic disc neovascularization in juvenile rheumatoid arthritis. Am J Ophthalmol 1990;110:210–212.
8. Pach JM, Herman DC, Garrity JA, Kalina PH. Disc neovascularization in chronic anterior uveitis. Am J Ophthalmol 1991;111:241–243.
9. Kalina PH, Pach JM, Buettner H, Robertson DM. Neovascularization of the disc in pars planitis. Retina 1990;10:269–273.
10. Tugal-Tutkun I, Onal S, Altan-Yaycioglu R, Altunbas HH, Urgancioglu M. Uveitis in Behçet disease: an analysis of 880 patients. Am J Ophthalmol 2004;138:373–380.
11. Atmaca LS, Batioglu F, Idil A. Retinal and disc neovascularization in Behçet's disease and efficacy of laser photocoagulation. Graefes Arch Clin Exp Ophthalmol 1996;234:94–99.
12. Atmaca LS. Fundus changes associated with Behçet's disease. Graefes Arch Clin Exp Ophthalmol 1989;227:340–344.
13. Atmaca LS. Experience with photocoagulation in Behçet's disease. Ophthalmic Surg 1990;21:571–576.
14. International Study Group for Behçet's Disease. Evaluation of diagnostic ('classification') criteria in Behçet's disease: toward internationally agreed criteria. Lancet 1990;335:1078–1080.
15. Tugal-Tutkun I, Urgancioglu M. Childhood-onset uveitis in Behçet disease: a descriptive study of 36 cases. Am J Ophthalmol 2003;136: 1114–1119.
16. Kötter I, Zierhut M, Eckstein AK, et al. Human recombinant interferon α-2a for the treatment of Behçet's disease with sight threatening posterior or panuveitis. Br J Ophthalmol 2003;87: 423–431.
17. De Andrea M, Ravera R, Gioia D, Gariglio M, Landolfo S. The interferon system: an overview. Eur J Paediatr Neurol 2002;6 Suppl A:A41–A46.
18. Ezekowitz AB, Mulliken JB, Folkman J. Interferon α-2a therapy for lifethreatening hemangiomas of infancy. N Engl J Med 1992;326: 1456–1463.
19. Stuebiger N, Koetter I, Zierhut M. Complete regression of retinal neovascularisation after therapy with interferon α in Behçet's disease. Br J Ophthalmol 2000;84:1437–1438.
20. Sfikakis PP, Kaklamanis PH, Elezoglou A, et al. Infliximab for recurrent, sight-threatening ocular inflammation in Adamantiades-Behçet disease. Ann Intern Med 2004;140:404–406.
21. Giansanti F, Barbera ML, Virgili G, Pieri B, Emmi L, Menchini U. Infliximab for the treatment of posterior uveitis with retinal neovascularization in Behçet disease. Eur J Ophthalmol 2004;14:445–448.

shown that treatment with levodopa may improve the vision in patients with recent onset NAION,[6] but the results are not conclusive.[7]

In TON, the optic nerve is indirectly injured by a concussive force to the head. The IONTS results show that no clear benefit is obtained by either corticosteroid therapy or optic canal decompression surgery.[3]

Thus, other treatment modalities are needed to treat the damaged optic nerve in cases of NAION and TON. It was recently reported that electrical stimulation of the spiral ganglion cells is effective in preserving their function in cases of deafness.[8,9] Also, it has been reported that electrical stimulation promotes the speed of motor axonal regeneration in rats.[10] Studies in our laboratory have shown that the survival of retinal ganglion cells in the rat eye after axotomy of the optic nerve is significantly increased if electrical stimulation is applied to the optic nerve just after axotomy in adult rats.[11] In addition, transcorneal electrical stimulation (TES) with a bipolar (concentric rings) contact lens electrode has been shown to stimulate the retinal ganglion cells and/or their axons.[12,13]

In light of these results, we investigated the efficacy and safety of TES as a method of improving and preserving the function of the optic nerve fibers in eyes of patients with NAION or TON.

Methods

Patients

These studies were performed at the Osaka University Medical School, Osaka, Japan. Three consecutive patients with NAION and five consecutive patients with TON were studied between March 2003 and June 2004. The exclusion criteria were visual acuity ≥0.4, a follow-up period of <3 months, use of a cardiac pacemaker, and the presence of corneal or retinal diseases. Patients with NAION who had an erythrocyte sedimentation rate of >30 mm/h or a C-reactive protein (CRP) value of >6 mg/dl were also excluded.

The eight patients were treated by TES after informed consent was obtained, and in full compliance with the regulations of the institutional review board. The procedures used conformed to the tenets of the Declaration of Helsinki.

The pretreatment best-corrected visual acuity (BCVA) ranged from 0.01 to 0.2 (median, 0.2) in the NAION patients, and from hand motion (HM) to 0.2 (median, 0.05) in the TON patients. The fellow eye of all patients was normal except in patient 3. The age of the patients ranged from 57 to 75 years (median, 61 years) in the NAION group, and 14 to 71 years (median, 16 years) in the TON group. The interval between the visual loss and the time of the TES treatment was 4 to 24 months (median, 6 months) in the NAION group, and 3 weeks to 11 months (median, 4 weeks) in the TON group. The follow-up period was 3 to 18 months (median, 7 months) (Table 1).

Figure 1. Schematic diagram of the transcorneal electrical stimulating (TES) system (*left*). Photograph showing the Burian-Allen (B-A) contact lens electrode in place (*right*). The retina was stimulated electrically by the electrodes embedded in the B-A electrode using biphasic pulses.

Interventional Procedures

Patients were treated according to the following protocol. The cornea was anesthetized with 0.4% oxyburocaine hydrochloride, and covered with 3% hyaluronic acid and 4% chondroitin sulfate (Viscoat, Alcon Japan, Tokyo, Japan) to prevent injury from the contact lens electrode. A bipolar contact lens Burian-Allen(B-A) electrode (Hansen Ophthalmic Laboratories, Iowa City, IA, USA) was placed on the cornea, and electric current pulses (20 pulses) were delivered from a stimulator (Nihon Koden, Tokyo, Japan) and a stimulus isolation unit (WPI, Sarasota, FL, USA) through two concentric electrodes embedded in the contact lens (Fig. 1).

Initially, the current of the biphasic pulses (duration, 10 ms; frequency, 20 Hz; number, 20) was increased from 300 μA to 2 mA to determine the threshold current necessary to elicit the phosphenes, which were perceived in both the peripheral and central visual area. The electrical stimuli were delivered continuously for 30 min using biphasic pulses after the phosphenes became visible.

Assessment of Outcome

For functional assessments, BCVA was determined using a standardized Landolt visual acuity chart, and the visual field was determined by kinetic Goldmann perimetry and the value of the critical flicker fusion frequency (CFF). These tests were performed by certified orthoptists who were unaware of the TES protocol. The visual acuity was converted to logMAR units. HM visual acuity was set at 2.9 logMAR units.[4] An improvement of ≥0.3 logMAR units between the pre- and posttreatment visual acuities was considered to be an improvement of visual acuity, while a decrease of >0.3 logMAR units was considered to be a worsening.

For quantitative evaluation of the peripheral visual field, the area of the visual field including the V/4 isopter

Table 1. Patient characteristics

Patient no.	Age/Sex	Dx	Duration	Time	BCVA	CFF Hz	GP V/4 area	GP Max ISP	Curr of Tx (μA)
1	66/F	NAION	6 m	pre	0.2	14	7.3	I/3	700
				1 m	0.2	16	7.5	I/2	
				3 m	0.5	36	4.5[b]	I/2	
2	57/M	NAION	24 m	pre	0.01	0	4.1	V/4	750
				1 m	0.02	11	14.8[a]	I/4	
				3 m	0.02	11	12.1[a]	I/3	
3	75/F	NAION	4 m	pre	0.2	22	12.2	I/3	600
				1 m	0.3	20	10.8	I/2	
				3 m	0.2	25	13.5	I/2	
4	14/M	TON	3 w	pre	0.05	38	13.7	I/2	650
				1 m	0.07	44	15	I/2	
				3 m	0.08	43	13.3	I/2	
5	24/M	TON	11 m	pre	0.15	30	2.4	I/2	750
				1 m	0.3	33	2.8	I/2	
				3 m	0.2	33	2.2	I/2	
6	71/M	TON	3 m	pre	0.2	18	9.4	I/2	700
				1 m	0.2	16	10.4	I/2	
				3 m	0.2	20	9.6	I/2	
7	14/M	TON	4 w	pre	0.02	19	6.3	I/4	800
				1 m	0.05	27	10.8[a]	I/2	
				3 m	0.05	33	10.8[a]	I/2	
8	16/M	TON	3 w	pre	HM	0	1.4	V/4	800
				1 m	HM	9	1.4	I/4	
				3 m	0.02	10	2.3[a]	I/3	

M, male; F, female; Dx, diagnosis; NAION, nonarteritic ischemic optic neuropathy; TON, traumatic optic neuropathy; Duration, duration from the onset to treatment; Time, time of examination; pre, pretreatment; m, months after treatment; w, weeks after treatment; BCVA, best-corrected visual acuity; GP, Goldmann perimetry; V/4 area, the area of the V/4 isopter (10^3 deg^2); Max ISP, the most sensitive isopter; Curr of Tx, current intensity of treatment; CFF, critical flicker fusion frequency; HM, hand motion.

[a] V/4 area enlarged ≥20% compared with the pretreatment value.

[b] V/4 area decreased ≥20% compared with the pretreatment value.

was determined from the Goldmann perimeter using the Scion Image program (Scion, Frederick, MD, USA). Because the variation in the quantified area of the normal fellow eyes in seven patients (patient 3 excepted) was less than 20% (data not shown), we defined an improvement of the peripheral visual field to have occurred when the area of the poststimulation visual field increased by ≥20%, while a worsening was considered to have occurred when the area decreased by ≥20%. An improvement of the central visual field was also considered to have occurred when a more sensitive isopter was found after the treatment.

The value of CFF was determined by averaging the frequency of flicker appearance and disappearance. Because the variation of CFF in the normal fellow eyes in seven patients (patient 8 excepted) was less than 15% (data not shown), we defined an improvement of the CFF to have occurred when the area of poststimulation CFF increased by ≥15%.

The visual acuity and visual field testing were performed before and 1 and 3 months after TES.

To assess the safety of TES, the anterior segment of the eyes was examined by slit-lamp biomicroscopy to determine whether corneal epithelial defects had been induced, whether there were alterations in the size and symmetry of the pupils, and whether there were cells or flare in the anterior chamber. These examinations were performed immediately after the treatment and on the day following TES, as well as at 1 and 3 months posttreatment. The intraocular pressure (IOP) and fundus were also examined on the day following treatment. Thereafter, the eyes were examined at 1 and 3 months after TES. The number of corneal endothelial cells was counted 3 months after treatment and compared with the pretreatment value.

Results

The BCVA at 3 months after treatment was improved by ≥0.3 logMAR units in six eyes (two NAION eyes and four TON eyes) and was unchanged in the remaining two eyes (one NAION and one TON; Fig. 2). At 3 months after TES, the area of the peripheral visual field improved significantly in three eyes (one NAION and two TON), was unchanged in four eyes (one NAION and three TON), and worsened in one eye (NAION). A more sensitive isopter appeared at 3 months after treatment in five eyes (three NAION and two TON), but did not appear in the other three eyes (zero NAION and three TON). None of the eyes lost the initial isopter (Figs. 3, 4).

The CFF at 3 months after treatment was improved by ≥15% in five eyes (two NAION and three TON) and was

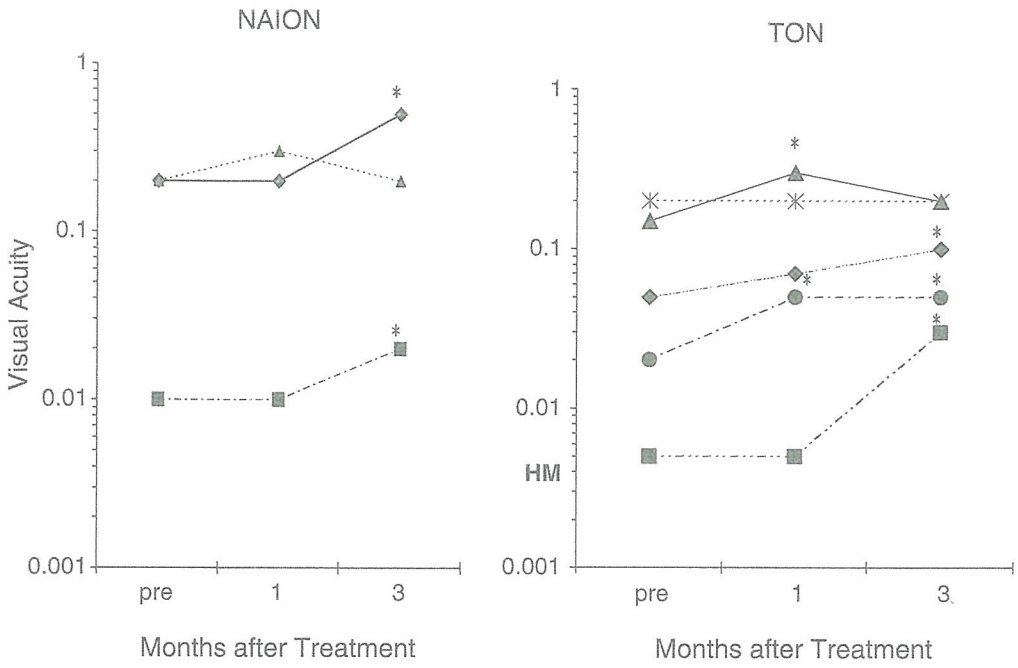

Figure 2. Effect of TES on visual acuity. Change in visual acuity after TES in eyes with nonarteritic ischemic optic neuropathy (*NAION*) (*left*) or traumatic optic neuropathy (*TON*) (*right*). *, improvement of vision by ≥0.3 log minimum angle of resolution(logMAR) units compared with the pretreatment value; *pre*, denotes pretreatment value; *HM*, hand motion. —/◆, Case 1; –·–/■, Case 2; ·····/▲, Case 3; –·–·–/◆, Case 4; —/▲, Case 5; ·····/✳, Case 6; – · –/●, Case 7; –·–/■, Case 8

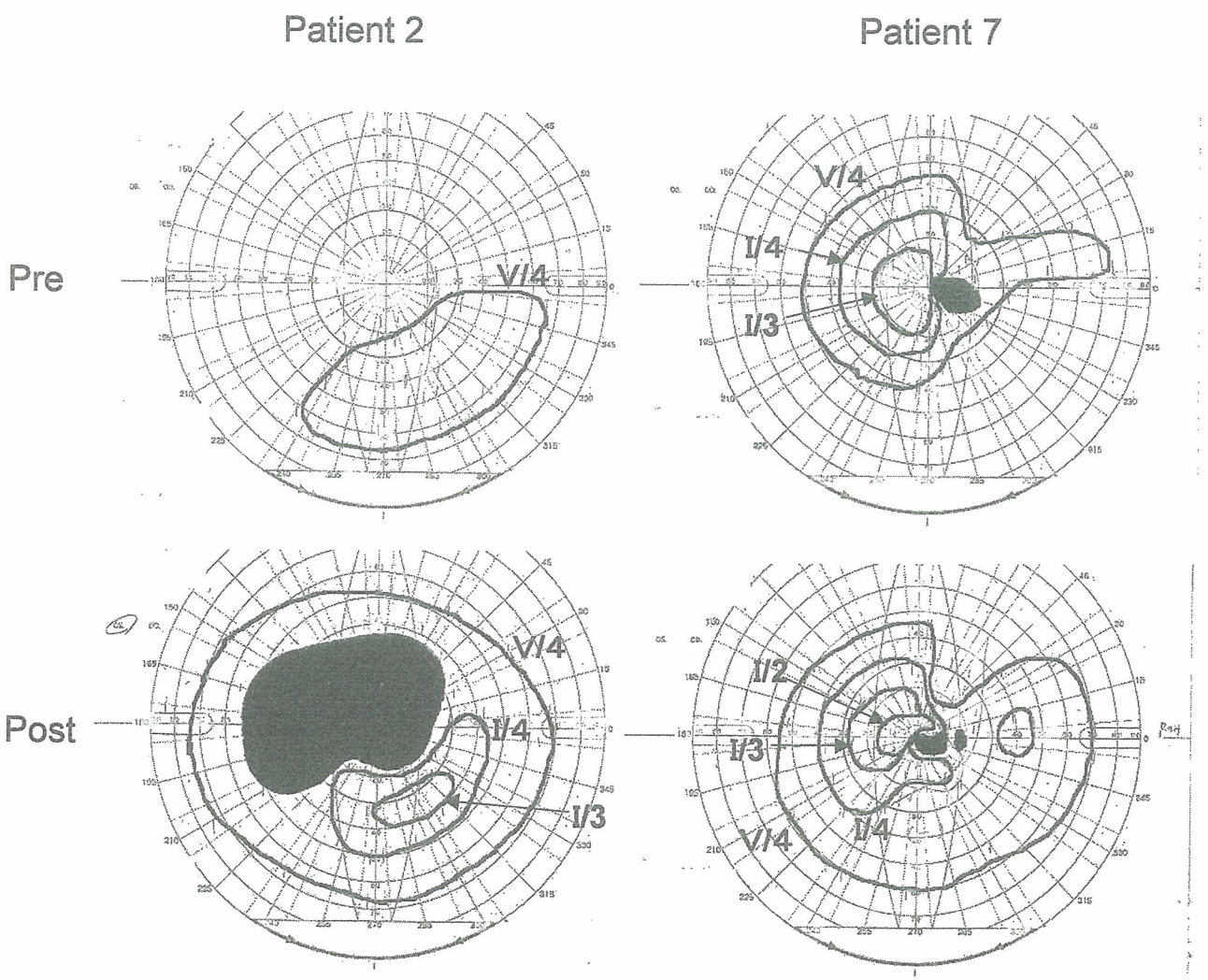

Figure 3. Visual fields. The Goldmann visual fields of patient 2 (NAION, *left*) and patient 7 (TON, *right*) before (*top*) and after (*bottom*) treatment. After treatment, the isopter of the peripheral visual field (V/4) enlarged, and more sensitive isopters (I/4 and I/3 in patient 2 and I/2 in patient 7) were detected.

Jpn J Ophthalmol
Vol 50: 266–273, 2006

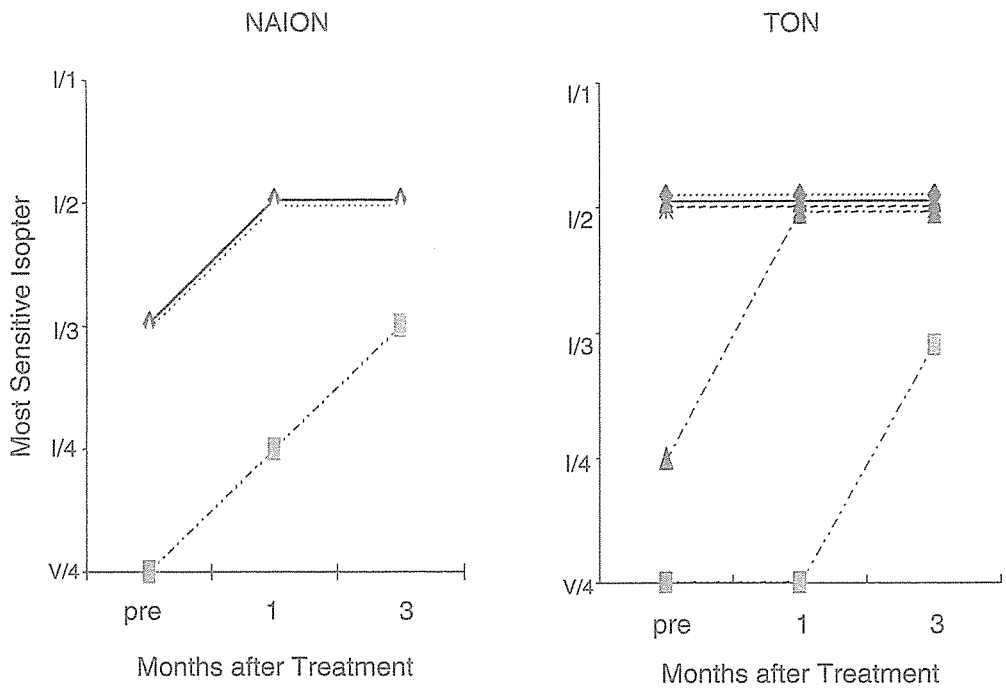

Figure 4. Appearance of more sensitive isopters in the NAION group (*left*) and the TON group (*right*). In all three patients with NAION and in two of the five patients with TON, more sensitive isopters appeared 1 to 3 months after treatment. *I/1* denotes the most sensitive isopter, followed by *I/2*, *I/3*, and *I/4*. *V/4* denotes the isopter of the peripheral visual field. —/◆, Case 1; – –/■, Case 2; ·····/△, Case 3; —·—/◆, Case 4; – –/▲, Case 5; —/※, Case 6; – · –/▲, Case 7; —·—/■, Case 8

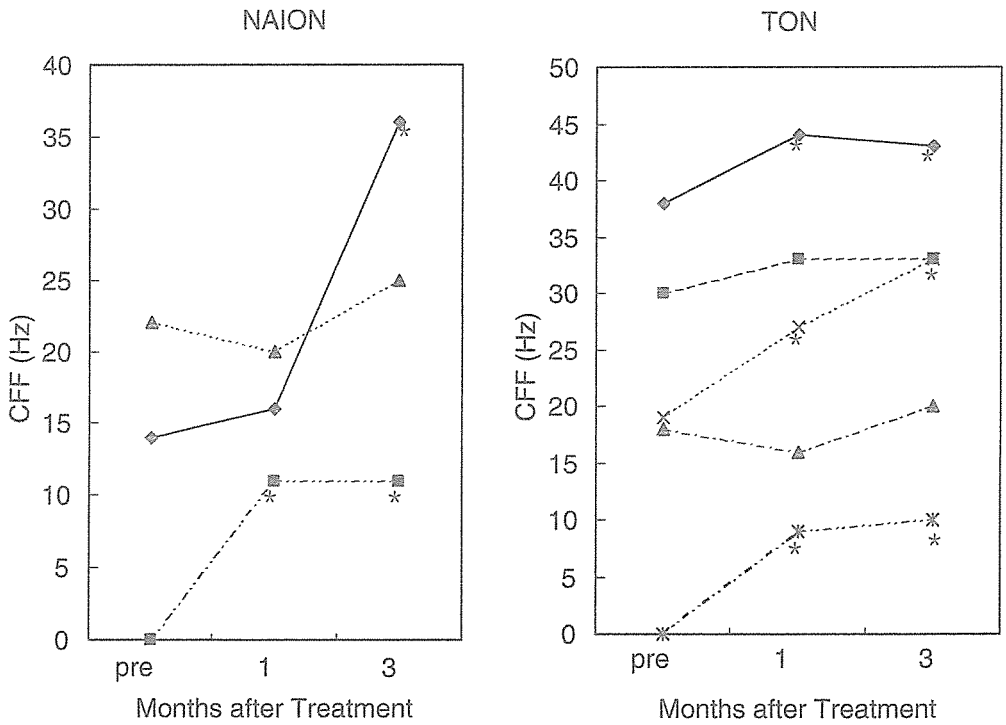

Figure 5. Effect of TES on critical flicker fusion frequency (*CFF*) Change of CFF after TES in eyes with NAION (*left*) and *TON* (*right*). *denotes an improvement of CFF by 15% or more compared with the pretreatment value. —/◆, Case 1; – –/■, Case 2; ·····/▲, Case 3; —/◆, Case 4; ----/■, Case 5; – –/▲, Case 6; – · –/×, Case 7; —·—/※, Case 8

unchanged in the remaining three eyes (one NAION and two TON; Fig. 5).

None of the patients reported experiencing pain during the TES treatment. A mild superficial punctuate keratopathy was observed in all eyes after the treatment, which healed by the next day in all eyes (Fig. 6). The number of corneal endothelial cells had not changed significantly in any of the eyes at 3 months, compared with the number before treatment.

The size and shape of the pupil was unchanged in all eyes, and no cells or flare was observed in the anterior chamber of any eyes just after the treatment or on the next

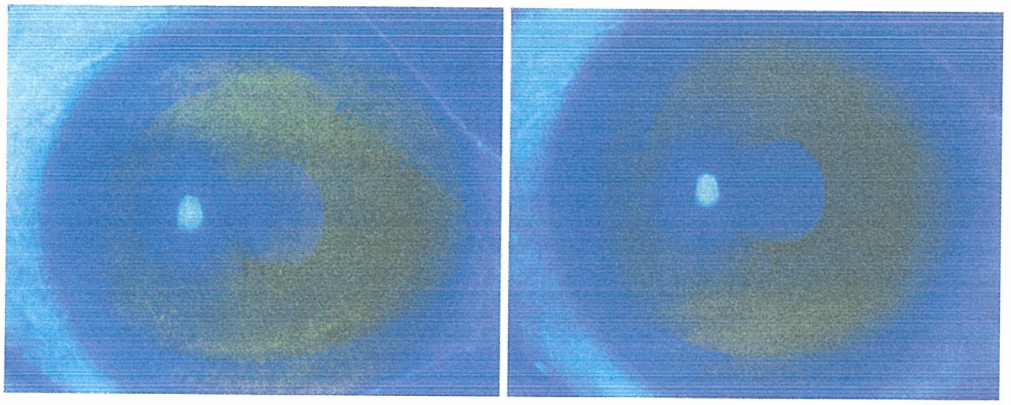

Figure 6. Photographs of the cornea of patient 1 stained with fluorescein dye, taken just after treatment (*left*) and on the following day (*right*). A superficial punctuate keratopathy was observed just after treatment, but was not present the next day.

day. The IOP did not change, and fundus examinations showed no change in the retina or optic disc on the day following treatment.

Case Report

A 64-year-old woman (patient 1) noticed a sudden loss of the inferior visual field in her left eye on 14 November 2002. She was referred to us the next day, and her BCVA was RE, 1.0 and LE, 0.5. A relative afferent pupillary defect was present in her left eye. Ocular fundus examination showed optic disc edema in the left eye (Fig. 7), and fluorescein angiography showed hypoperfusion in the upper temporal disc area (Fig. 6). The CRP value was normal (<2.5 mg/dl). She did not have pain during eye movements, and magnetic resonance imaging did not show changes in the optic nerve. From these results, she was diagnosed with NAION in the left eye. Oral aspirin and vitamin B12 were prescribed.

The BCVA in her left eye decreased to 0.15 in December but recovered to 0.2 in January 2003 and remained unchanged for 5 months. In May 2003, TES was performed on the left eye (600 μA, 20 Hz, 30 min), and the BCVA improved to 0.4 in June and to 0.5 in August. However, the BCVA decreased again to 0.3 in September and to 0.1 in December. TES was performed again in March 2004 (700 μA, 20 Hz, 30 min), and the BCVA improved to 0.2 in April and to 0.3 in June (Fig. 7).

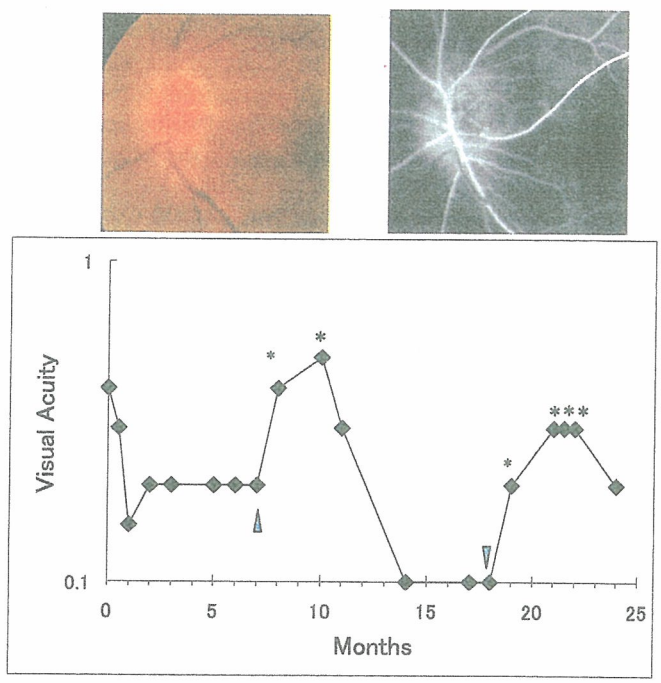

Figure 7. Fundus photograph (*top left*) and early-phase fluorescein angiogram (FA) (*top right*) of the left eye of patient 1 at the first visit. Papilledema of moderate degree can be seen. FA shows hypoperfusion in the upper temporal disc area. The time course of the best corrected visual acuity (BCVA) in the left eye (*bottom*). *Arrowhead* denotes the day of TES treatment. *denotes the improvement of BCVA ≥0.3 logMAR units from the pretreatment value.

Discussion

The visual acuity and CFF improved in two of the three eyes in the NAION group, while the other eye showed no change. In these three eyes, a more sensitive isopter was detected in the visual field after TES (Figs. 2, 4, 5). The IONDT study showed that the mean visual acuity improved up to 3 months after the onset of NAION,[2] and did not improve thereafter during the 24-month follow-up period. Thus, we conclude that TES treatment was effective in some eyes with NAION even if the TES treatment was performed more than 4 months after the onset of NAION.

Our case report shows that in a patient whose visual acuity was stable for more than 5 months, TES can still improve the visual acuity at 3 months after the treatment. Although the visual acuity decreased 6 months later, after a second TES treatment, the vision improved again (Fig. 7). These findings strongly suggest a causal relationship between the treatment and the visual improvement.

Our case report also shows the limitation of a single TES treatment, because the recovery of vision was obtained for only 3 months, suggesting that repeated treatments might be necessary to maintain the improved vision.

Johnson et al.[6,14] showed that levodopa improved the visual function in 30% of patients with NAION, even if they were treated more than 6 months after the decrease of vision,[14] and in 75% of patients if treated within 2 weeks of the onset of NAION.[6] Therefore, we believe that earlier TES treatment will be more beneficial for the recovery of visual acuity in NAION patients.

This theory is supported by the results in eyes with TON. Three months after TES, the BCVA and CFF improved in all three eyes treated within 4 weeks after onset (patients 4,7,8) but did not improve in the two eyes treated 3 months or more after onset (patients 5, 6; Fig. 2). However, the possibility of spontaneous recovery cannot be ruled out.[15] A randomized controlled study is necessary to confirm the efficacy of TES treatment for TON.

The effective level of electric current for the TES treatment was determined to be the threshold for eliciting phosphenes in both peripheral and central visual fields. This level was selected because it would assure the activation of most retinal ganglion cells and their axons.

Several mechanisms have been proposed to explain the neuroprotective effect of electrical stimulation.[10,16,17] We have demonstrated that insulin-like growth factor 1, a neurotrophic factor, is gradually upregulated in the rat retina up to 2 weeks after TES.[18] This may explain why a single TES treatment is effective in improving vision for up to 3 months. However, additional laboratory studies are necessary to determine more conclusively the mode of action of the electrical stimulation.

To the best of our knowledge, this is the first application of TES for the treatment of optic neuropathy, and we considered it very important to test its safety. The effects of using the Burian-Allen contact lens for the TES treatment are comparable to those following its use for electroretinographic recordings. Only mild corneal punctuate keratopathy was observed after TES treatment in all eyes, and the keratopathy healed by the next day (Fig. 6). The safety of TES on the corneal epithelium may stem from the protective effect of hyaluronic acid and chondroitin sulfate, as well as the balanced charge stimulation using biphasic pulses.

Because the current delivered by the contact lens electrode also stimulated the ciliary body, we carefully checked the size and shape of the pupils, and whether cells or flare was present in the anterior chamber. No significant alterations were observed. The electrical current may also penetrate the cornea, so we confirmed that there were no changes in the corneal endothelium. In particular, no changes were observed in the number of corneal endothelial cells. These observations suggest that TES is a safe method for stimulating the retinal ganglion cells and their axons.

In conclusion, TES led to the improvement of the visual acuity in eyes of some patients with NAION or TON. However, a larger prospective, randomized clinical trial with controls is necessary to confirm conclusively the effectiveness of TES treatment.

Acknowledgments. The authors are grateful to Dr. Yozo Miyake, Dr. Satoshi Suzuki, Dr. Yutaka Fukuda, Dr. Tomomitsu Miyoshi, and Dr. Hiroyuki Kanda for valuable discussions on the development of a system for transcorneal electrical stimulation. This study was partly supported by Health Science Research grants from the Ministry of Health, Labor, and Welfare, Japan, and by a grant from the Ministry of Education, Sports, Culture, Science, and Technology (No. 16591752). T. Morimoto was supported by the Japan Society for the Promotion of Science Research Fellowship for Young Scientists.

References

1. Trobe JD. The neurology of vision. New York: Oxford University Press; 2001. p. 215–218.
2. The Ischemic Optic Neuropathy Decompression Trial Research Group. Ischemic optic neuropathy decompression trial. Twenty-four-month Update. Arch Ophthalmol 2000:118;793–798.
3. Levin AL, Beck RW, Joseph MP, Seiff S, Kraker R, and the International Optic Nerve Trauma Study Group. The treatment of traumatic optic neuropathy. Ophthalmology 1999;106:1268–1277.
4. Lessel S. Nonarteritic anterior ischemic optic neuropathy. Enigma variations. Arch Ophthalmol 1999;117:386–388.
5. The Ischemic Optic Neuropathy Decompression Trial Research Group. Optic nerve decompression surgery for nonarteritic anterior ischemic optic neuropathy (NAION) is not effective and may be harmful. JAMA 1995;273:625–632.
6. Johnson LN, Guy ME, Krohel GB, Madsen RW. Levodopa may improve vision loss in recent-onset, nonarteritic anterior ischemic optic neuropathy. Ophthalmology 2000;107:521–526.
7. Lee AG, Brazis PW. Clinical pathways in neuro-ophthalmology. An evidence-based approach. 2nd ed. New York: Thieme; 2003. p. 82–83.
8. Miller JM, Altschuler RA. Effectiveness of different electrical stimulation conditions in preservation of spiral ganglion cells following deafness. Ann Otol Rhinol Laryngol 1995;166:57–60.
9. Leake PA, Hradek GT, Snyder RL. Chronic electrical stimulation by a cochlear implant promotes survival of spiral ganglion neurons after neonatal deafness. J Comp Neurol 1999;412:543–562.
10. Al-Majed AA, Brushart TM, Gordon T. Electrical stimulation accelerates and increases expression of BDNF and trkB mRNA in regenerating rat femoral motorneurons. Eur J Neurosci 2000; 12:4381–4390.
11. Morimoto T, Miyoshi T, Fujikado T, Tano Y, Fukuda Y. Electrical stimulation enhances the survival of axotomized retinal ganglion cells in vivo. Neuroreport 2002;13:227–230.
12. Potts AM, Inoue J. The electrically evoked response of the visual system (EER). Invest Ophthalmol 1968;7:269–278.
13. Miyake Y, Yanagida K, Yagasaki K. Clinical application of EER (electrically evoked response). (1) Analysis of EER in normal subjects. Nippon Ganka Gakkai Zasshi (Acta Soc Ophthalmol Jpn) 1980;84:354–360.
14. Johnson LN, Gould TJ, Krohel GB. Effect of levodopa and carbidopa on recovery of visual function in patients with nonarteritic anterior ischemic optic neuropathy of longer than six months' duration. Am J Ophthalmol 1996;121:77–83.
15. Berestka JS, Rizzo JF. Controversy in the management of traumatic optic neuropathy. Int Ophthalmol Clin 1994;34:87–96.
16. Franklin JL, Sanz-Rodriguez C, Juhasz A, Deckwerth TL, Johnson EM. Chronic depolarization prevents programmed cell death of

sympathetic neurons in vitro but does not support growth: requirement for CA2+ influx but not Trk activation. J Neurosci 1995; 15:643–664.
17. Miller AL, Prieskorn DM, Altschuler RA, Miller JM. Mechanism of electrical stimulation-induced neuroprotection: effects of verapamil on protection of primary auditory afferents. Brain Res 2003;966:218–230.
18. Morimoto T, Miyoshi T, Matsuda S, et al. Transcorneal electrical stimulation rescues axotomized retinal ganglion cells by activating endogenous retinal IGF-1 system. Invest Ophthalmol Vis Sci 2005;46:2147–2155.

Jpn J Ophthalmol 2006:50:274–276
DOI 10.1007/s10384-005-0305-x

BRIEF COMMUNICATION

Prevalence of Glaucoma in Adults with Down's Syndrome

Tomoko Yokoyama[1], Hiroki Tamura[1], Hidetoshi Tsukamoto[1], Kiyoko Yamane[2], and Hiromu K. Mishima[1]

[1] Department of Ophthalmology and Visual Science, Graduate School of Biomedical Sciences, Hiroshima University, Hiroshima, Japan; [2] Department of Pediatrics, Hiroshima Child Guidance Center for Mental and Physical Disabilities, Hiroshima, Japan

Abstract

Purpose: To compare the prevalence of glaucoma in adults with Down's syndrome (DS) to that in non-DS control adults.

Methods: Twenty-six patients (14 men and 12 women) with DS and 188 control subjects (105 men and 83 women) were studied. The mean age was 35.1 ± 6.9 (± SD) years in the DS group and 36.9 ± 5.2 years in the control group. There were no significant differences in age or sex distribution between the two groups. Glaucoma was diagnosed by two glaucoma specialists based on the optic disc findings obtained through dilated pupils.

Results: The prevalence of patients with glaucoma in the DS group was 11.5%, significantly higher (P = 0.014) than that in the control group, 1.1%. There was no significant difference in intraocular pressure between glaucomatous eyes (12.2 ± 3.2 mmHg) and nonglaucomatous eyes (11.1 ± 4.1 mmHg) in the DS group (P = 0.465).

Conclusions: The prevalence of glaucoma in adult patients with DS was significantly higher than that in age-matched control subjects. **Jpn J Ophthalmol** 2006;50:274–276 © Japanese Ophthalmological Society 2006

Key Words: Down's syndrome, glaucoma, neurodegenerative disease, prevalence

Introduction

Glaucoma is a degenerative disease of the optic nerve caused by various factors. Recently, glaucoma has been reported to be associated with systemic neurodegenerative diseases such as Alzheimer's disease and Parkinson's disease; the prevalence of glaucoma in patients with Alzheimer's disease is 24.5%, and that in patients with Parkinson's disease is 23.7%.[1]

Patients over the age of 30 years with Down's syndrome (DS) tend to develop neuropathological changes similar to those in Alzheimer's disease.[2] The prevalence of glaucoma in children with DS has been reported to be somewhat low by several studies.[3,4] Recently, the life expectancy of patients with DS has been extended; however, the prevalence of glaucoma in adults with DS has not been reported. Therefore, we evaluated the prevalence of glaucoma in adult patients with DS and compared the results with age-matched control subjects.

Subjects and Methods

Twenty-six adult patients with DS (14 men, 12 women), who were recruited from six institutions in Hiroshima, Japan, underwent ophthalmologic examinations in June and July 2003. The ages of the patients ranged from 22 to 56 years (mean, 35.1 years). Patients who had had retinal surgery or vitreous surgery were excluded, but those who had had cataract surgery were included.

Received: July 19, 2005 / Accepted: October 20, 2005
Correspondence and reprint requests to: Hidetoshi Tsukamoto, Department of Ophthalmology and Visual Science, Graduate School of Biomedical Sciences, Hiroshima University, 1-2-3 Kasumi, Minami-ku, Hiroshima 734-8551, Japan
e-mail: htsuka@hiroshima-u.ac.jp

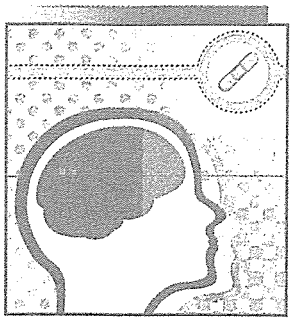

©EYEWIRE

Silicon LSI-Based Smart Stimulators for Retinal Prosthesis

A Flexible and Extendable Microchip-Based Stimulator

BY JUN OHTA, TAKASHI TOKUDA, KEIICHIRO KAGAWA, TETSUO FURUMIYA, AKIHIRO UEHARA, YASUO TERASAWA, MOTOKI OZAWA, TAKASHI FUJIKADO, AND YASUO TANO

Neural electronic stimulators play an important role in neuroscience and clinical neuroengineering. Stimulators are now commercially available, while others continue to be developed [1]–[11]. As examples in clinical neuroengineering, stimulators have been applied to cochlear prostheses [12], [13] and retinal prostheses [14]–[20]. In this article, we focus on retinal prosthesis as schematically shown in Figure 1. In the configuration, the implanted stimulator is placed upon the suprachoroid; this stimulation method is called STS (suprachoroidal transretinal stimulation) [21], [22].

The stimulator includes several electrodes that stimulate the retinal cells electrically and evoke a spatial phosphen pattern. Thus, the number of the electrodes is considered to be important, although at the present time, only a small number of stimulus electrodes have been realized. Creating devices with over 1,000 electrodes is challenging; such a large number of connections between electrodes and external lead wires are extremely difficult to fabricate.

Recently, neural interface devices based on silicon microelectronics or large-scale-integration (LSI) have emerged [23]–[38]. Since LSI allows the integration of smart functions such as control, amplification, and signal processing with the stimulators, LSI-based neural interface devices are attracting significant interest. To solve the interconnection issue, we have proposed the introduction of LSI technologies to retinal prosthesis devices [39]–[48]. In addition to solving the interconnections issue, LSI-based stimulators bring several advantages to photosensors for subretinal implantation. We have studied LSI-based stimulators for STS [47], [48], subretinal implantation [39]–[44], and epiretinal implantation [45].

There are many technical challenges to overcome when applying LSI-based neural interface devices to retinal prosthesis. First, the LSI-based interface must be biocompatible. A standard LSI structure is not at all suitable in a biological environment; silicon nitride is conventionally used as a protective top layer in standard LSIs but is eroded in a biological environment. Second, the stimulus electrodes must be compatible with the standard LSI structure; aluminum is conventionally used for wire-bonding pads in standard LSIs but is completely inadequate as a stimulus electrode for neural cells because aluminum dissolves in saline solution. Third, in addition to the electrode material, the shape of the electrode affects the efficiency of stimulation, with a convex shape being suitable for efficient stimulation. Consequently, we need to develop a completely new packaging technology that fits into a standard LSI structure, is biocompatible, and is effective in stimulating neural cells. Finally, the devices must also be thin and flexible to fit the anatomy of target organs and to avoid damaging tissues. However, silicon, the base material of the LSI chip, is so rigid that thinning of the LSI chip increases the risk of breakage. We have previously demonstrated that an image sensor made of silicon thinner than 50 μm can be bent and can operate with sufficient accuracy [41]. Such a thinned LSI chip, however, must be handled very carefully. To overcome the issue of mechanical rigidity and to realize a feasible LSI-based neural interface device, we have proposed a device architecture consisting of silicon (Si)-based microchips that cooperatively operate under a single set of control signals [46]–[48].

In this article, we report on a retinal prosthesis smart stimulator that is biocompatible and fully compatible with a standard LSI structure and that provides high-stimulation efficiency. Our stimulator is based on multimicrochip architecture. We have specifically developed the stimulator for retinal prostheses, but it could be applied to other neuroscience and clinical neuroengineering fields.

Si-LSI Based Stimulator: Operation Principle and Fundamental Characteristics

Circuit Design Issues

To stimulate retinal cells effectively, biphasic current pulse stimulation is generally preferred [49]. In addition, biphasic pulses are required to maintain the charge balance of the biological environment [50]. When such stimulation is implemented using standard LSI technology, a necessary consideration is that the output current and voltage range must stay within the limits of the technology. That is, the output current must stay within about -500 to $+500\,\mu$A and the voltage from slightly below 0 V to the power supply voltage V_{dd} of the LSI technology used; for example, using standard 0.6-μm CMOS (complementary metal oxide semiconductor) technology, the range is from -0.5 to $+5.5$ V. It is noted that when we use a biphasic current pulse, the reference voltage

0739-5175/06/$20.00©2006IEEE

We need to develop a completely new packaging technology that fits into a standard LSI structure, is biocompatible, and is effective in stimulating neural cells.

V_{ref} is usually set at half of the full swing of voltage range in the system used, and, therefore, the voltage swing in one polarity must be less than $0.5 \times V_{dd}$. For example, for $V_{dd} = 5$ V, the positive voltage swing must be less than 2.5 V. Consequently, it is necessary to design an LSI that can output enough high pulse current amplitude in the voltage range in a biological environment such as saline solution.

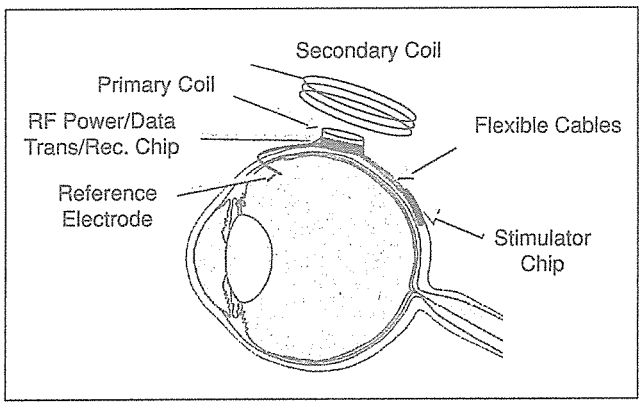

Fig. 1. The conceptual drawing of a retinal prosthesis. The implanted chip is placed upon the suprachoroid in this case (47).

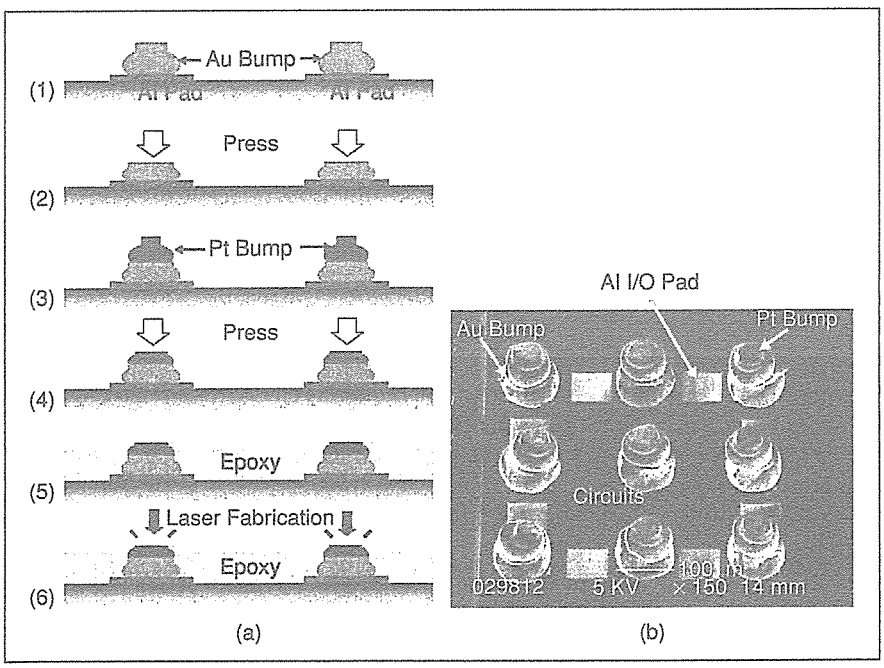

Fig. 2. Pt/Au stacked bump electrodes on an LSI chip. (a) Fabrication process flow: (1) gold bump forming, (2) pressing of gold bump, (3) platinum bump forming, (4) pressing of platinum bump, (5) molding, and (6) platinum exposure. (b) SEM photograph (48).

Electrodes and Packaging

The electrodes and packaging technologies used in the design of a standard LSI-based stimulator are now described. Figure 2(a) shows the fabrication process for our electrode [47], [48]. First, a platinum/gold (Pt/Au) stacked bump structure is formed on an aluminum (Al)-bonding pad in a standard LSI chip. Aluminum cannot be used in the biological environment, but platinum is a suitable electrode material due to its excellent biocompatibility and charge injection efficiency [51]–[53]. The platinum electrode juts out of the top surface of the chip to enable close contact with neural cells. To make this jutting platinum electrode, we have formed the stacked bump in two steps, in which a gold bump is initially formed and a platinum bump is formed on top. The gold bump acts as a cushion for the hard platinum bump; direct formation of the platinum bump sometimes breaks the LSI I/O pad.

After fabrication of the stacked Pt/Au bump, the entire LSI chip, including the bonding wires, is covered with a biocompatible epoxy resin. Finally, the resin on top of the electrodes is completely removed using a high-power argon (Ar) ion laser; thus the entire LSI chip, except for the top of the platinum electrodes, is covered with resin. Parylene coating can be additionally applied to the resin to ensure durability in the biological environment and can also be removed by the Ar ion laser.

Figure 2(b) shows a scanning electron micrograph (SEM) of the stacked Pt/Au bump electrodes fabricated on an LSI chip. The diameter of the structure is about 100 μm and can be controlled by changing the silver and platinum wire diameter. We have obtained good reproducibility in fabricating over 100 such bump electrodes using an automatic bump bonder. The coating has been confirmed to protect the interior of the LSI chip, including the area close to the electrodes, from the biological environment. It is noted that other high-efficiency, biocompatible electrode materials such as iridium oxide (IrO_x) and titanium nitride (TiN) [54], [55] can be deposited on the platinum bump.

Operation in Saline Solution

To assess the applicability of the electrodes and packaging technologies, we operated the fabricated stimulator in a saline environment. The stimulator

Our smart LSI-based stimulator is effective in stimulating retinal cells.

chip was fabricated in 0.6-μm standard CMOS technology. The chip formed with a Pt/Au stacked bump electrode was wire-bonded to a test board and was molded. Then the coating on the platinum electrode was removed by an excimer laser to leave an exposed area with a diameter of about 20 μm, by the process described above. A reservoir of saline solution was formed around the chip. Figure 3(a) shows the processed chip on the test board with the reservoir. The details of the circuits are described in a later section.

The molded chip was dipped in saline solution and the reference voltage $V_{ref} = 1.5$ V was supplied via an silver/silver chloride (Ag/AgCl) reference electrode. The biphasic pulse parameters are the amplitudes of the cathodic and anodic currents, I_c and I_a, and the pulse durations of the anodic, cathodic, and interpulses, t_c, t_i, and t_a. In this work, we fixed $|I_c| = I_a$. The pulse durations t_c, t_i, and t_a were set to the same value. Hence, the biphasic pulse waveform can simply be described by the amplitude and interval, for example, 100 μA/100 μs.

Figure 3(b) shows the measured operational voltage for three biphasic, current-controlled pulses. The pulse parameters used are shown in the figure. Similar reports on neural stimulation using platinum electrodes suggest that the trace presented in Figure 3(b) is reasonable for a cathodic-first biphasic charge injection [51], [52]. In Figure 3(b), the operational voltage lies within the voltage swing of the chip (from −0.5 to +5.5 V for the present device) for typical conditions in retinal cell stimulation experiments. This indicates that the LSI chip can output sufficient biphasic current pulses to stimulate retinal cells.

Another consideration relates to the electrochemical aspect of current injection into a biological environment. Current injection from an electrode into saline (or other biological solution) includes electrochemical reactions at the interface. Excess voltages applied to the interface cause irreversible chemical reactions such as electrolysis and the formation of bubbles [52], [53]. The current injection for neural stimulation needs to be carried out without causing irreversible electrolysis or bubbles. The current injection capability depends on the material and surface structure of the electrode. In our experiments, we have confirmed in electrochemical experiments using platinum electrodes that the voltage for appropriate current injection swings within the safe range for reversible electrochemical processes. In addition, we observed no bubbles on the platinum electrodes during current injection. Consequently, we conclude that the present packaging of Pt/Au stacked bump electrodes is applicable for neural stimulation.

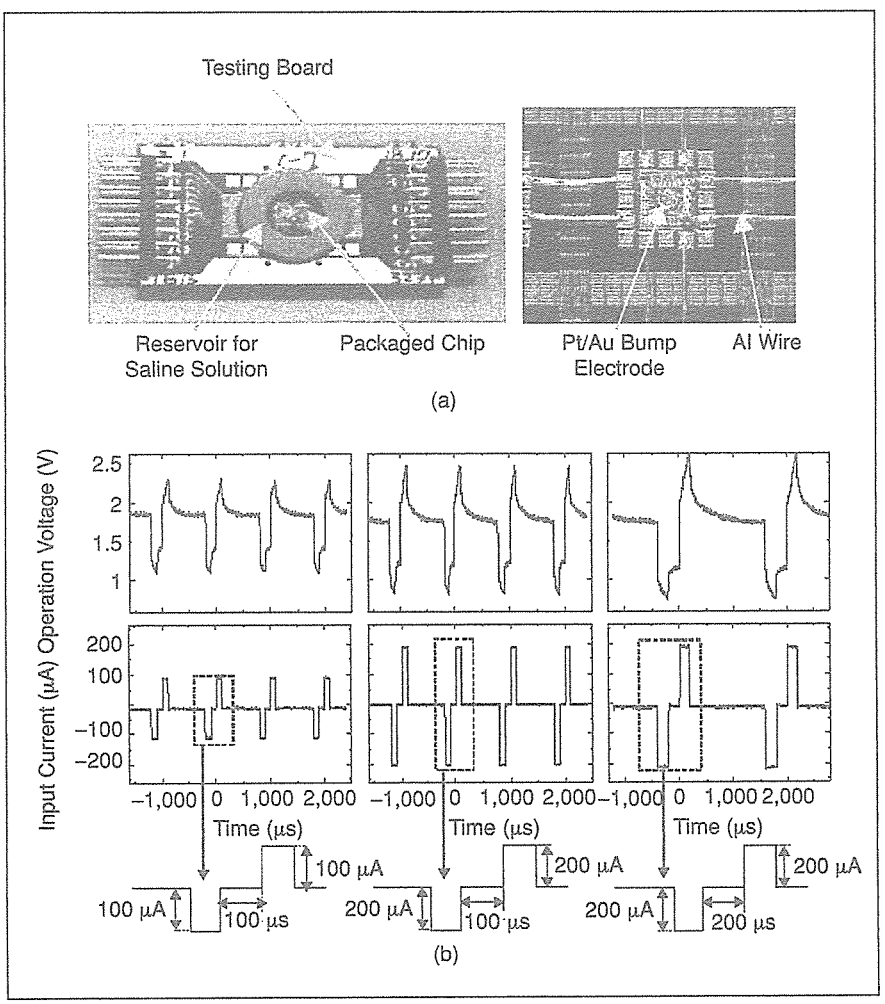

Fig. 3. Current injection experiments of Pt/Au stacked bump electrodes in a saline environment (48). (a) A packaged LSI chip on a testing board for experiments in a saline environment. (b) Oscilloscope traces of current stimulation in a saline solution. Upper and lower traces show voltages of electrodes and injection current, respectively.

Stimulation of Frog Retina with a Smart LSI-Based Stimulator

Electrical Stimulation Using a Smart LSI-Based Stimulator

In the previous section, we demonstrated the successful operation of the LSI stimulator in saline solution. In this section, we show that our smart LSI-based stimulator is effective in stimulating retinal cells. We used detached bullfrog retinas as the in vitro experiment [44]. The stimulator used was a CMOS image sensor-based stimulator array we have developed for retinal prostheses [43], [44]. Table 1 summarizes the chip specifications.

The chip has two functions, which can be switched; an externally controlled stimulator and a stimulator that is controlled by input light intensity such as in photoreceptor cells. A current source and pulse shape circuits are integrated on the chip (the details are described in [43], [44]). The Pt/Au stacked bump electrode and chip molding processes were performed as described in the previous section. Before molding, the chip was bonded onto a printed circuit board for handling. A reservoir of Ringer solution was placed surrounding the chip.

A piece of the bullfrog retina (about 3–5 mm in width) was placed, with the retinal ganglion cell (RGC) side face up, on the surface of the packaged chip. Figure 4(a) shows the experimental setup. Electrical stimulation was performed using the chip at a selected single pixel. A tungsten counter electrode with a tip diameter of 5 μm was placed on the retina and, thus, a transretinal current was produced between the counter electrode and the chip electrode. A top-view photograph of

Table 1. Chip specifications.

Technology		0.6 μm standard 2-poly 3-metal CMOS
Number of pixels		16 × 16
Pixel size		240 μm × 240 μm
Power supply voltage		3 V (logic), 5 V (stimulus)
Stimulus electrode size		About 100 μm ϕ
Stimulus current	Range	−1 to +1 mA (biphasic)
	Resolution	exponent: 3-b; significand: 3-b

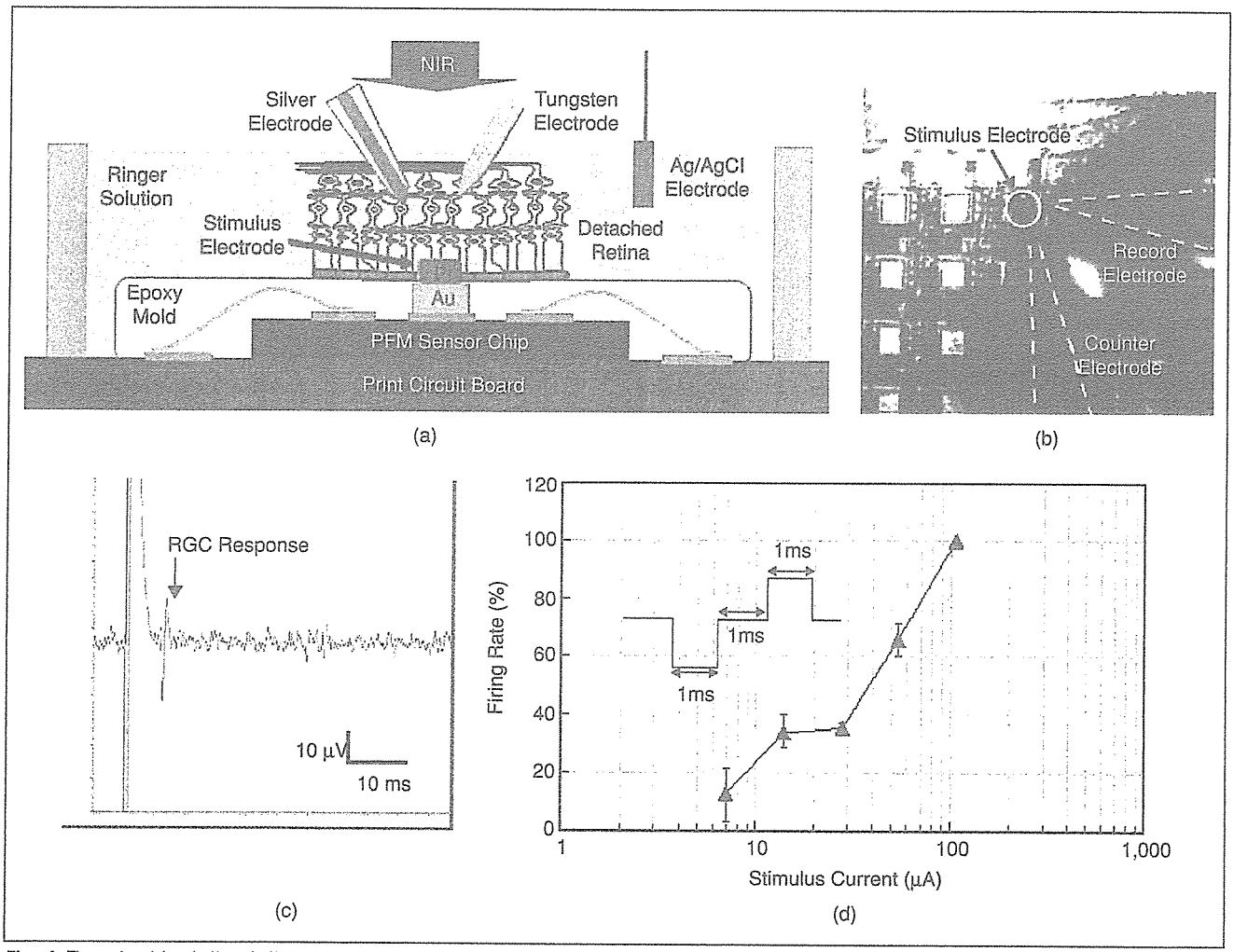

Fig. 4. The electrical stimulation of a detached retina with the fabricated LSI-based stimulator (44). (a) Experimental setup, (b) a microphotograph of the experiment, (c) an example of the RGC response waveform, and (d) the firing rate of the RGC as a function of the stimulus pulse amplitude.

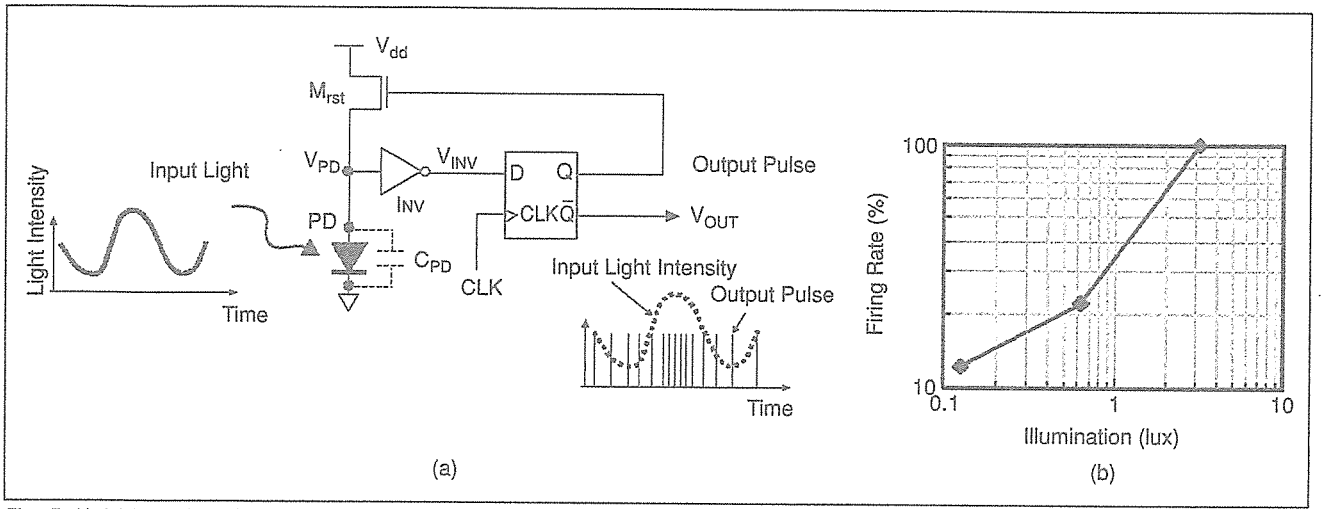

Fig. 5. Light-to-pulse stimulation: (a) the schematic of a PFM photosensor and (b) the firing rate of RGCs as a function of the input NIR light intensity (44).

the experimental setup is shown in Figure 4(b). We used a cathodic-first biphasic current pulse. Stimulus pulses were generated with the chip for $t_c = t_i = t_a = 1$ ms and $I_a = |I_c|$. A silver electrode with a diameter of 50 μm was used to record the extracellular response of the RGCs. An Ag/AgCl wire was used for the reference electrode.

We have previously examined the firing rate of the RGC response [44]; Figure 4(c) shows an example of the RGC response waveform obtained. We have confirmed that the firing rate increases in response to input light intensity as shown in Figure 4(d). This demonstrates the effectiveness of the developed electrodes, which are compatible with the standard LSI structure.

Light-to-Pulse Stimulation

The chip is integrated with an image sensing function; that is, the input light intensity is converted into pulse trains with the pulse frequency proportional to the input light intensity. This device, known as a *pulse-frequency-modulation (PFM) photosensor* [56], is suitable for stimulating retinal cells. We were the first to propose that a PFM-based photosensor could be applied to a retinal prosthesis device [39]. The schematic of a PFM photosensor is shown in Figure 5(a). The operation principle is briefly described as follows. The node voltage V_{PD} decreases by discharging the parasitic capacitance C_{PD} through the photocurrent, and eventually, when V_{PD} reaches the threshold voltage of the inverter V_{th}, the inverter turns on, resets the transistor M_{rst}, and finally charges C_{PD}, which is the initial state. The D-FF (flip-flop) acts as a delay element. The pulse is output when the inverter chain turns on and results in a pulse frequency that is proportional to the input light intensity. We have already fabricated and demonstrated PFM photosensors [39]–[41] and have analyzed their operation theoretically [42]. Such a photosensor could be applied to subretinal implantation and has been recently studied by other researchers [57].

Subsequently, we have tested this PFM function in stimulation of the detached frog retina. The experimental setup is the same as for electrical stimulation except for an additional input of near-infrared (NIR) light. Note that NIR light

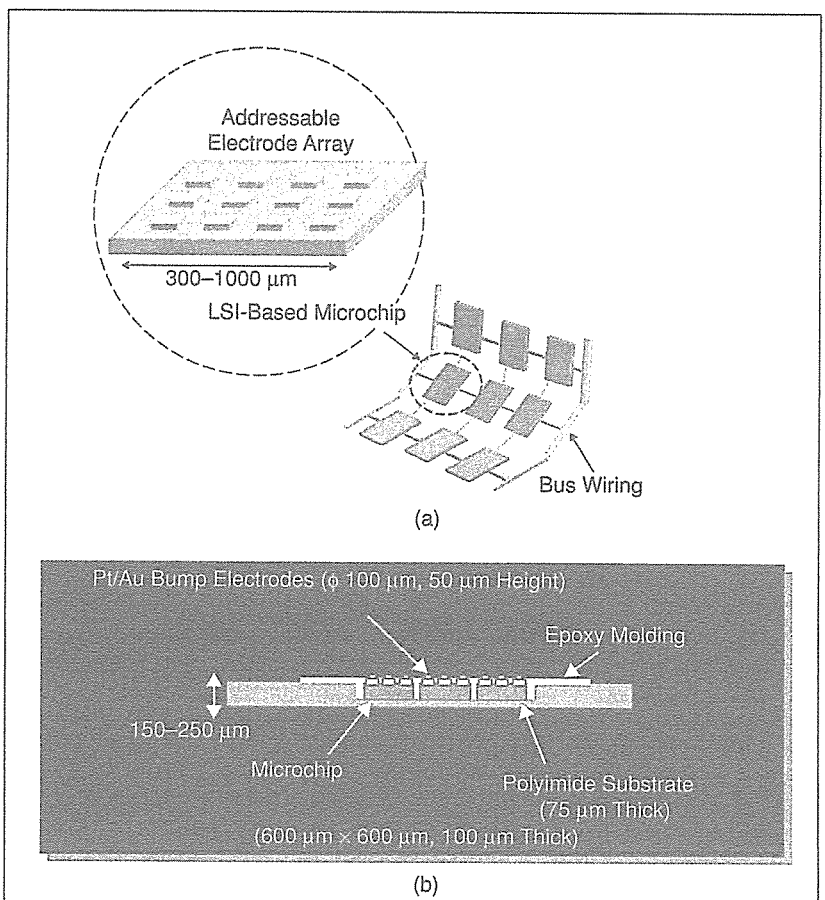

Fig. 6. A conceptual drawing of the smart distributed LSI-based microchip array (4). Each microchip has stimulus electrodes: (a) a schematic of the entire array and (b) a cross-sectional view.